RASĀYAN *J. Chem.*
Vol. 19 | No. 3 | 1781-1786 | July-September | 2026
ISSN: 0974-1496 | e-ISSN: 0976-0083 | CODEN: RJCABP
http://www.rasayanjournal.com
http://www.rasayanjournal.co.in

DESIGN, CRYSTAL STRUCTURE, DFT AND MOLECULAR DOCKING STUDIES OF SCHIFF BASE DERIVED FROM ALIPHATIC DIAMINE

V. Palani, P. Shakila, and M. Santhana raj prabhu✉
Department of Chemistry, Muthurangam Government Arts College (Autonomous), Affiliated to Thiruvalluvar University, Vellore-632002, (Tamil Nadu) India
✉Corresponding author: msrgcr@gmail.com

ABSTRACT

In the modern era, cancer has become a major health problem due to increasing environmental pollution. The purpose of this research is to create a new chemical that can fight against cancer cells. We introduced a Schiff base synthesised from *m*-nitrobenzaldehyde and 1,3-diaminoisopropanol. The compound (HL-2SB) was elucidated by using UV-Vis, IR, NMR, HRMS and SCXRD. SCXRD confirms that the HL-2SB is a monoclinic crystal with space group ($P2_1/n$) system. FMO analysis of the compound gave a HOMO-LUMO gap of 4.4216 eV, indicating their kinetic stability and reactivity. From DFT studies, the large electrophilicity index (6.1879 eV) showed the ability to resist electron removal, efficient charge transfer and stability in structure. The molecular docking studies of HL-2SB with 8RY2 protein the strong hydrogen bonds between them. These studies reveal that the compound acts as an anticancer agent.

Keywords: Schiff Base, *m*-Nitrobenzaldehyde, 1,3-Diaminoisopropanol, Molecular Docking, Anticancer.
RASĀYAN*J. Chem.*, Vol. 19, No. 3, 2026

INTRODUCTION

In recent years, Schiff bases have gained significant attention in the biological field, which includes antimicrobial, anti-inflammatory, antitubercular, antiviral and anticancer properties. Thakur *et al.* showed that the viral research on Schiff bases against COVID-19, HIV and Chikungunya on both molecular docking (*in vitro* and *in silico*).[1] Fiertek *et al.* reported metal complexes of Schiff bases as a potent agent to treat breast cancer.[2] Gosu Nageswara Reddy *et al.* reported Schiff bases of Cu and La metal complexes and their antimicrobial properties for the treatment of infectious diseases.[3] Güngör *et al.* reported Schiff bases and their antifungal and antibacterial activities.[4] In this study, well focused on the synthesis of a Schiff base from aliphatic diamine and substituted benzaldehyde and their anticancer activity.

EXPERIMENTAL

Material and Measurements

Chemicals and reagents were sourced commercially and used as received. 1,3-diaminoisopropanol, *m*-nitrobenzaldehyde and other chemicals were from S.D. Fine Chemicals. FT-IR spectra recorded on Shimadzu, in the range of 4000-400 cm^{-1}. ^1H NMR were recorded on FEI-TECNAL, G2-20 TWIN (Operating voltage 200 kV) with $CDCl_3$ as solvent and TMS as an internal reference, UV recorded on Specord 210 plus spectrometer, SCXRD recorded on Bruker D8 QUEST FIXED CHI diffractometer, DFT performed by Gaussian 09 software.

General Procedure

About 3.35g (22mmol) of *m*-nitrobenzaldehyde was treated with 1.0 g (11 mmol) 1,3-diaminoisopropanol using 15 mL of ethanol as a solvent. The reaction was maintained under stirring at RT for 25-30 minutes, after monitoring by TLC, the absence of reactants confirmed the formation of Schiff base (HL-2SB). A crude colourless solid precipitated out, which was filtered, washed with hot ethanol, dried and recrystallised. Quality crystals were obtained in ethanol within a couple of weeks. Yield: 89%, m.p. 98 ^oC, soluble in MeOH, $CHCl_3$, DMF, DMSO and CH_3CN. Representation of HL-2SB is shown in Fig.-1.

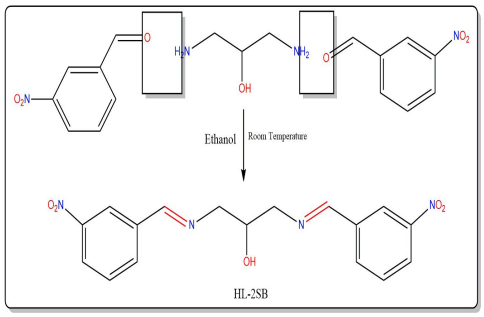

Fig.-1: Scheme of HL-2SB

RESULTS AND DISCUSSION

IR (KBr, cm^{-1}): 3285 cm^{-1} (O-H, hydroxyl), 1645 cm^{-1} (- C = N -, imine), 2846 – 2901 cm^{-1} (-C-H, aliphatic), 1344 and 1358 cm^{-1} (*sym*. str., NO_2) and 1532 cm^{-1} (*asy*. str., NO_2). The IR data confirmed the formation of imine functionality in HL-2SB from the aldehyde and primary amine.

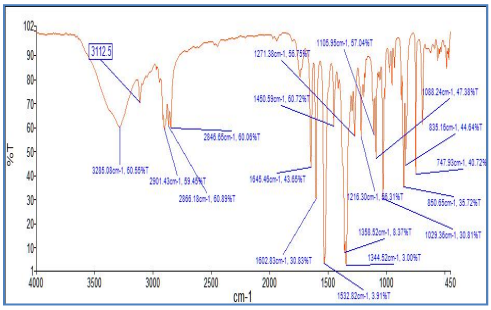

Fig. 2: FT-IR of HL-2SB

UV-Vis (λ_{max}, nm): Two absorbance maxima obtained. One at 207 nm shows aromatic systems or unsaturated groups due to $\pi \rightarrow \pi^*$ transition in the HL-2SB. Another one at 241 nm indicates the $n \rightarrow \pi^*$ transition due to the presence of hetero atoms like N and O in HL-2SB.

^{1}H NMR &^{13}C NMR: δ 3.835–3.992 ppm (m, 5H) =N–CH_2CH(OH)CH_2-N= (aliphatic protons), 5.71 ppm (s, 1H) – CH(OH)-(hydroxyl proton), 8.484 ppm (s, 2H) –HC=N- (imine protons), 8.404 – 8.279 ppm (m, 8H) aromatic protons (Fig.-3). 64.93 ppm (Carbon of aliphatic methylene), 123.47 – 149.18 ppm (Carbon of aromatic ring), 149.18 and 160.95 ppm (aromatic Carbon attached to NO_2). The NMR data confirm the framework of the molecule contains aliphatic, aromatic, nitro and imine groups (Fig.-4).

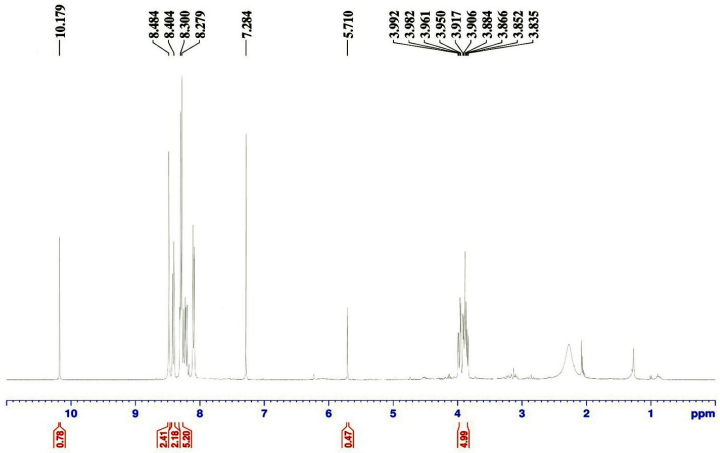

Fig.-3: ^{1}H NMR of HL-2SB

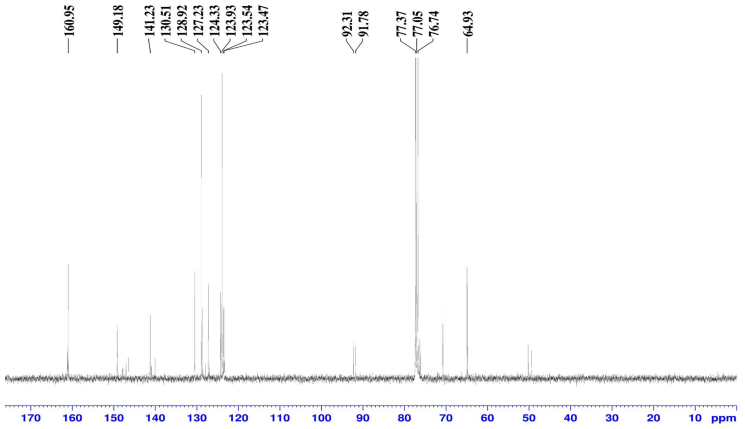

Fig.-4: ^{13}C NMR of HL-2SB

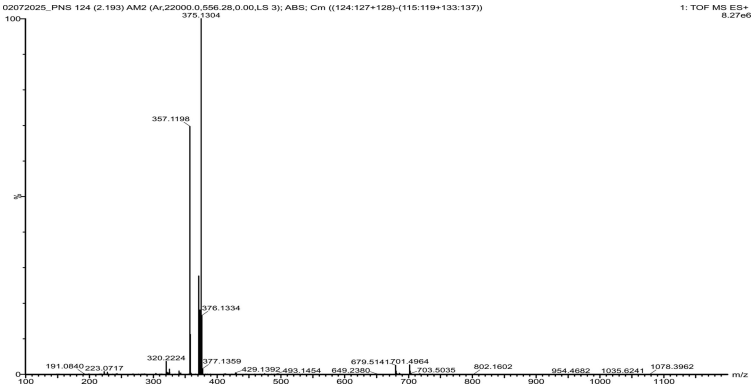

Fig. 5: HRMS of HL-2SB

HRMS: $[M+H]^+$= 357.11 m/z (cal.356.34 m/z), which is in perfect agreement with the calculated m/z.
SCXRD: A colourless, needle-shaped crystal. The Crystal data were deposited with CCDC 2503144.

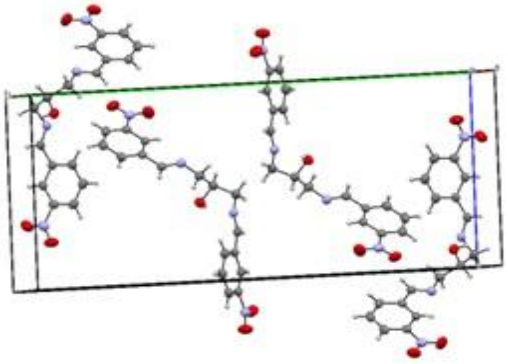

Fig.-6: Crystal Packing of the HL-2SB

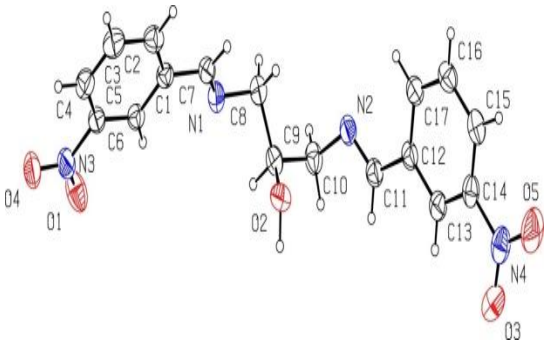

Fig.-7: Atom Labelling Scheme of HL-2SB

Table-1: Experimental SCRXD Data for HL-2SB

	CCDC Number	2503144	
Molecular Formula	$C_{17}H_{16}N_4O_5$	Molecular weight	356.34
Temperature [K]	300(2)	Space group & Crystal system	$P2_1/n$ (14), Monoclinic
α [°] = γ [°]	90	β [°]	93.8080(10)
a, *b* and *c* (10^{-10}m)	4.86170(10), 29.1737(9) and 11.8296(4)	size [mm^3]	0.058×0.089×0.398
Appearance	Colorless	Crystal shape	Needle
2θ range [°]	3.72 to 56.58 (0.75 Å)	Radiation	Mo K_α (λ=0.71073 Å)

Z	4	Volume [Å^3]	1674.13(8)
ρ_{calc} [g/cm^3]	1.414	M	0.107 mm^{-1}
F(000)	744		
h, k, l ranges	$-6 \le h \le 6$, $-38 \le k \le 38$, $-15 \le l \le 15$	Reflections collected	66838
Independent reflections	4165, R_{int} = 0.0681 R_{sigma} = 0.0307		
Data / Restraints / Parameters	4165 / 0 / 239	"Goodness-of-fit on F^2"	1.128
Final R indexes [$I \ge 2\sigma(I)$]	R_1 = 0.0500 wR_2 = 0.1148	Final R indexes [all data]	R_1 = 0.1116 wR_2 = 0.1626
Largest peak/hole [eÅ^{-3}]	0.20/−0.18	Extinction coefficient	0.0087(17)

HOMO-LUMO Analysis

FMO analysis provides significant insight into the electronic structure and reactivity of HL-2SB. The HOMO energy (–7.4415 eV) describes the electron-donating ability, whereas the LUMO energy (–3.0199 eV) indicates the electron-accepting tendency of the compound. The HOMO–LUMO energy gap of 4.4216 eV suggests moderate kinetic stability with controlled chemical reactivity. According to Koopmans' theorem, the ionisation potential (7.4415 eV) and electron affinity (3.0199 eV) are approximated from the negative values of HOMO and LUMO energies, respectively. The relatively high ionisation potential confirms resistance toward electron removal, while the positive electron affinity supports favourable electron acceptance. The global reactivity descriptors, including electronegativity (5.2307 eV) and chemical potential (–5.2307 eV), were evaluated based on conceptual density functional theory principles. The chemical hardness (2.2108 eV) reflects moderate resistance to charge transfer, and softness (0.2262 eV^{-1}) represents balanced polarizability. Furthermore, the electrophilicity index (6.1879 eV) indicates strong electrophilic character and enhanced electron-accepting capability.

MEP: The molecular electrostatic potential (MEP) surface of HL-2SB illustrates the three-dimensional charge distribution and identifies potential reactive sites within the molecule. The electrostatic potential values range from -6.142×10^{-2} a.u. (red region) to $+6.142 \times 10^{-2}$ a.u. (blue region), where the red regions belong to electron-rich zones and the blue regions show electron-deficient areas. The negative potential is predominantly localised over electronegative atoms, suggesting probable sites for electrophilic attack, while the positive regions are mainly distributed around hydrogen atoms and electron-poor centres, favouring nucleophilic interactions. The green areas represent regions of nearly neutral potential, indicating comparatively stable portions of the molecular framework. This variation in charge distribution confirms intramolecular charge transfer and polarisation effects within the system. The MEP surface is widely recognised as a reliable tool for predicting intermolecular interactions, hydrogen bonding tendencies, and reactive behaviour.[5] The observed electrostatic features are also consistent with density functional theory-based interpretations of chemical reactivity and molecular stability. Overall, the MEP analysis supports the presence of distinct electrophilic and nucleophilic regions, reinforcing the predicted stability and interaction capability of HL-2SB, as shown in the (Fig.-9).

Mulliken Atomic Charges

This study provides detailed insight into the electron density distribution within HL-2SB. The calculated charges reveal that the nitrogen atoms (N1 = –0.5281, N9 = –0.3141, N19 = –0.3164, and N27 = –0.5296) possess significant negative charge values, indicating strong electron-withdrawing character and their potential role as active sites for electrophilic interactions.[6] The oxygen atom (O28 = –0.3493) also exhibits a considerable negative charge, further confirming the localisation of electron density over electronegative atoms. In contrast, most hydrogen atoms show positive charge values ranging from 0.0693 to 0.2581, reflecting electron deficiency and their susceptibility toward nucleophilic attack. Among the hydrogen atoms, H52 (0.2581) and H50 (0.2330) display relatively higher positive charge values, suggesting stronger polarisation effects in their vicinity. Carbons such as C2 (0.2201) and C21

(0.2268) show positive character, whereas several aromatic carbons carry slight negative charges, supporting intramolecular charge transfer. The overall charge distribution pattern demonstrates significant polarisation within the molecule, which enhances intermolecular interaction capability. Furthermore, the localisation of negative charge over hetero atoms supports the predicted electrophilic behaviour, and the interaction potential of HL-2SB is shown in Fig.-10.

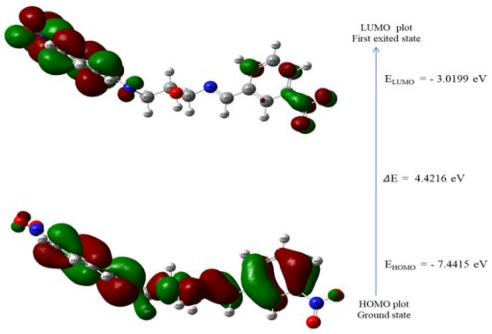

Fig.-8: FMO of HL-2SB

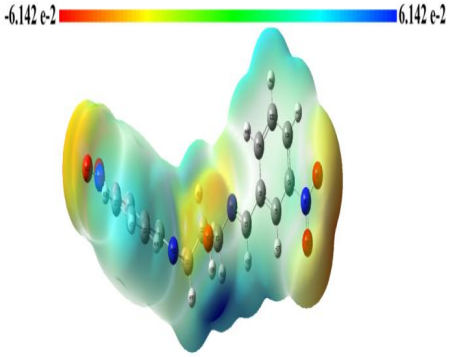

Fig.-9: MEP of HL-2SB

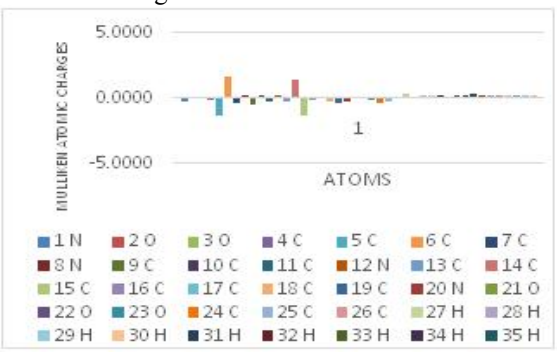

Fig.-10: The Histogram of Mulliken Atomic Charges of HL-2SB

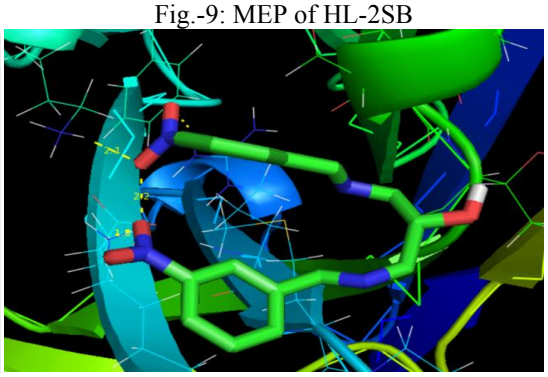

Fig.-11: 3D Interaction of 8YR2 Protein with HL-2SB

Molecular Docking Analysis

The molecular docking study of HL-2SB with the 8RY2 protein was carried out to check binding strength and interaction pattern in the active site. The 8RY2 crystal structure was obtained from the PDB (ID: 8RY2) and prepared appropriately before docking analysis.[7] The optimised ligand was docked into the active site region, and the most stable pose was selected based on the lowest binding energy and favourable interactions. The results indicate that HL-2SB forms three significant hydrogen bond interactions with amino acid residues LYS'63 (2.1 Å), LYS'43 (2.2 Å), and LEU'43 (1.8 Å), confirming strong and stable ligand–protein interactions within the acceptable hydrogen bonding distance range.

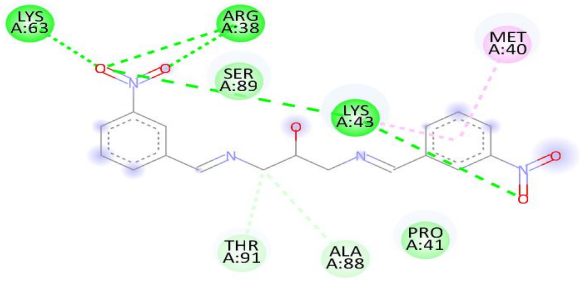

Fig.-12: 2D Structure of Hydrogen Bonding and Molecular Docking with Protein Target (8RY2)

The calculated binding energy of –5.96 kcal/mol suggests moderate binding affinity, while the intermolecular energy value of –8.64 kcal/mol confirms favourable van der Waals and electrostatic

contributions toward stabilisation of the complex. The estimated inhibition constant (Ki) of 42.89 µM indicates micromolar-level inhibitory potential against the 8RY2 anti-cancer target.[8] Hydrogen bonding plays a crucial role in anchoring the ligand within the receptor cavity and enhancing binding specificity. The RMSD value further supports the reliability of the predicted binding pose. Since 8RY2 corresponds to ANV419, an IL-2/anti-IL-2 antibody fusion protein developed for cancer immunotherapy, targeting this protein may contribute to immune modulation against tumour progression. Overall, the docking analysis demonstrates that HL-2SB exhibits stable accommodation within the active site of the 8RY2 protein and may serve as a promising candidate for further experimental validation in anti-cancer drug development.

CONCLUSION

The synthesized HL-2SB ligand has been characterised through spectral analysis, and SCXRD confirmed its molecular structure. DFT analysis revealed its electronic properties, while molecular docking with 8RY2 explored biological interaction. Mulliken charge analysis revealed electron density distribution, electrophilic behaviour, and interaction capabilities. Collectively, these findings highlight HL-2SB as a potential lead molecule for anticancer drug discovery, warranting further experimental validation.

ACKNOWLEDGMENTS

We acknowledge the scientific and technical assistance of the Single Crystal XRD facility supported jointly by DST and VIT under the DST-FIST scheme at VIT, Vellore.

CONFLICT OF INTERESTS

The authors declared that there is no conflict of interest.

AUTHOR CONTRIBUTIONS

The present work is related to SDG-3: *Good Health and Well-being*. All the authors contributed significantly to this manuscript, participated in reviewing/editing, and approved the final draft for publication. The research profile of the authors can be verified from their ORCID ids, given below:

V. Palani http://orchid.org/0009-0006-5890-4258
P. Shakila https://orcid.org/0009-0002-4752-7179
M. Santhana raj prabhu http://orchid.org/0009-0002-9814-459X

Cite this article as: V. Palani *et al.*, *Rasayan J. Chem.*, 19(3), 1781-1786(2026), https://doi.org/10.31788/RJC.2026.1939817

REFERENCES

1. Shalu Thakur, Ankita Jaryal, Aman Bhalla, *Results in Chemistry*, **7**, 101350(2024), https://doi.org/10.1016/j.rechem.2024.101350
2. Justyna Samaszko-Fiertek, Barbara Dmochowska, Janusz Madaj, *International Journal of Molecular Science,* **27(2)**, 678(2026), https://doi.org/10.3390/ijms27020678
3. G. N. Reddy, Venkatramana Losetty, C. Hazarathaiah Yadav, *Journal of Molecular Structure*, **1282**, 135161(2023), https://doi.org/10.1016/j.molstruc.2023.135161
4. Özlem Güngör, Perihan Gürkan, *Journal of Molecular Structure*, **1074**, 62(2014), https://doi.org/10.1016/j.molstruc.2014.05.032
5. T. Koopmans, *Physica*, **1(1-6)**, 104(1934), https://doi.org/10.1016/S0031-8914(34)90011-2
6. C. Arunagiri, M. Arivazhagan, A. Subashini, N. Maruthaiveeran, *Spectrochimica Acta Part A: Molecular and Biomolecular Spectroscopy,***131**, 647(2014), https://doi.org/10.1016/j.saa.2014.03.116
7. Helen M. Berman, John Westbrook, Zukang Feng, Gary Gilliland, T. N. Bhat, Helge Weissig, Ilya N. Shindyalov, Philip E. Bourne, *NucleicAcids Research*, **1**, 235(2000), https://doi.org/10.1093/nar/28.1.235
8. Nejeh Hannachi, Rim Elwej, Thierry Roisnel, Faouzi Hlel, *Scientific Research An Academic Publisher,* **13**, 1(2023), https://doi.org/10.4236/ojic.2023.131001

[RJC-9817/2026]